The habenula: an under-recognised area of importance in frontotemporal dementia?

INTRODUCTION

Behavioural variant frontotemporal dementia (bvFTD) is a neurodegenerative disorder characterised by atrophy of the frontal and temporal lobes and progressive behavioural and cognitive impairment. Some behavioural symptoms such as craving for food, alcohol or drugs, and hypersexuality are suggestive of abnormal reward processing. The reward circuit is formed by a number of different structures including the orbitofrontal cortex, ventral striatum (in particular the nucleus accumbens), ventral pallidum, anterior cingulate cortex, thalamus, hypothalamus, midbrain and habenula.[1] This complex network combines information about motivation, cognitive planning and motor control to develop an appropriate goal-directed response to external environmental stimuli. Many of the brain structures belonging to the reward circuit have been found to be atrophic in bvFTD,[2] supporting the theory that impairment of the reward system is an important factor in this disease. Among these structures, the habenula, found medial to the posterior thalamus, is uniquely positioned to participate in reward processing, acting as a convergence point for the limbic system and basal ganglia circuits,[3 4] and therefore playing a pivotal role in the integration of information required to generate goal-directed behaviours. Despite this key role, it has yet to be investigated in bvFTD.

The aim of this study was to investigate the volume of the habenula in a cohort of patients with bvFTD, hypothesising that it would be smaller than in healthy controls as well as an age-matched group of patients with Alzheimer's disease (AD) who typically do not show impairment of reward behaviour. We also hypothesised that the habenula would show comparable atrophy to other key areas in the reward network in bvFTD.

METHODS

Fifteen participants fulfilling criteria for the diagnosis of bvFTD (including eight with a *MAPT* mutation and four with a pathogenic expansion in the *C9orf72* gene) were recruited consecutively from a tertiary referral cognitive disorders clinic at the National Hospital for Neurology and Neurosurgery, London, UK. In total, 87% of the group were male with the mean (SD) age at onset 55.3 (8.9) years and disease duration 7.3 (3.8) years. Fifteen participants fulfilling criteria for typical AD (with early onset disease in order to match for age) were also recruited. Only 40% of the group were male with the mean (SD) age at onset 54.9 (4.5) years and disease duration 5.9 (2.7) years. Fifteen healthy controls (47% male) were also recruited. The mean (SD) age at scan was 62.6 (9.8) in bvFTD, 60.7 (5.9) in AD and 61.4 (8.9) in the controls, with no significant differences between the groups. Mini-Mental State Examination differed between the groups, being lowest in the AD group (20.4 (4.2)) then the bvFTD group (25.0 (4.6)) (AD vs bvFTD, p=0.011), both being lower than the control group (28.9 (1.3), p<0.001 and 0.055, respectively).

Segmentations of the habenula were performed manually on coronal slices of a volumetric T1-weighted MRI following a novel segmentation protocol adapted from previous descriptions[5 6] (see online supplementary data). We also calculated volumes for the rest of the brain using a cortical and subcortical parcellation as previously described,[7] (see online supplementary data). All brain volumes were corrected for total intracranial volume, which was calculated using SPM12 (http://www.fil.ion.ucl.ac.uk/spm).

Statistical analyses were performed in SPSS software V.22.0 (SPSS Inc, Chicago, Illinois, USA). Differences in demographic and cognitive features as well as brain volumes were tested with the Mann–Whitney U test for continuous variables and χ^2 test for dichotomous variables. For the brain volumes (30 comparisons), the Bonferroni correction for multiple comparisons was made so that only a threshold of p≤0.001 was considered significant.

RESULTS

The bvFTD group showed a 30% lower right and a 28% lower left habenular volume compared with controls (mean (SD) right: 16.4 (2.7) vs 23.3 (2.2) mm^3, left: 16.9 (2.4) vs 23.6 (2.2), p<0.0005, Mann-Whitney U test). The AD group
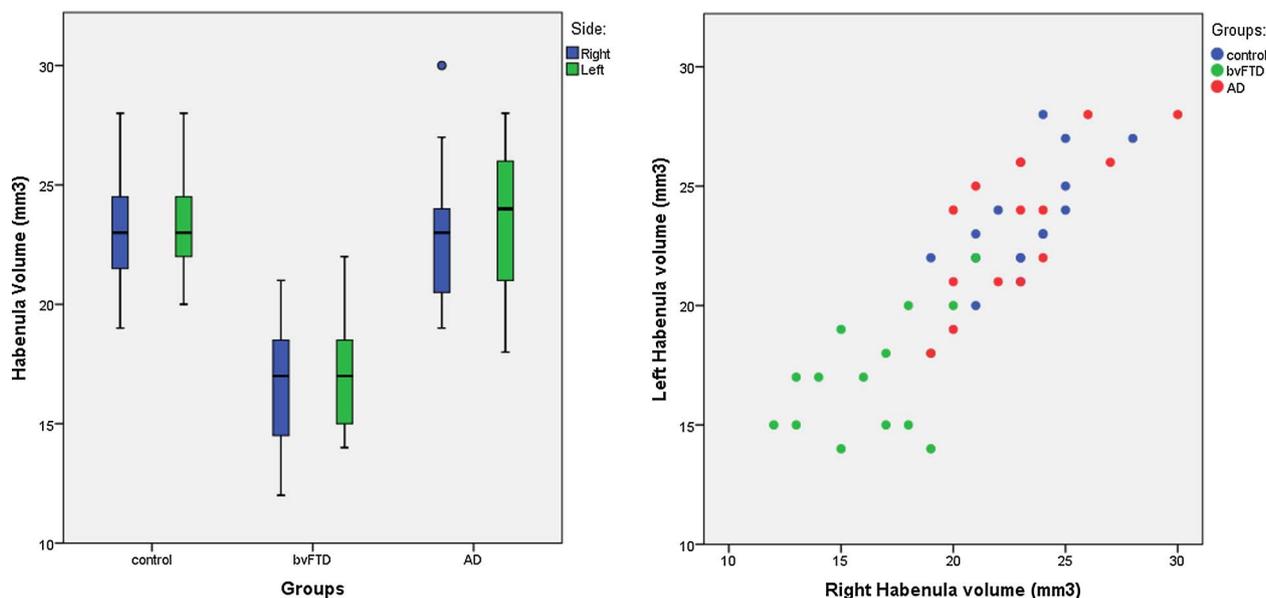
Figure 1 Volume of the left and right habenula (corrected for total intracranial volume) in 15 patients with behavioural variant frontotemporal dementia (bvFTD), 15 patients with Alzheimer's disease (AD) and 15 controls: (A) by group and (B) comparing the right and left side.

was not significantly different to controls (<1% difference): mean (SD) right: 23.0 (2.9), left: 23.6 (3.1), but the bvFTD group was significantly smaller than AD (right 29% and left 28% smaller, p<0.0005 for both sides) (figure 1).

No other cortical or subcortical region showed a larger percentage difference in volume in bvFTD compared with controls than the habenula (see online supplementary table). The insula cortex, amygdala, hippocampus and nucleus accumbens were the other most significantly involved regions, with volumes being 20% or smaller than controls. Other areas of the reward network including the frontal and cingulate cortices, and thalamus showed smaller volumetric differences compared with controls (see online supplementary table).

DISCUSSION

To the best of our knowledge, this is the first study investigating the habenula in bvFTD. Compared with healthy controls and patients with AD, bvFTD showed significantly smaller habenular volumes bilaterally. Furthermore, the habenula showed the largest percentage difference in volume in the bvFTD group compared with controls out of all of the cortical and subcortical regions measured. Similarly affected regions included the nucleus accumbens, amygdala, hippocampus and insula cortex, which form part of the reward network or are intrinsically linked to it. Other key areas of the reward network including the thalamus and brainstem were affected to a lesser extent. However, the key areas within the network form smaller parts of the regions

measured in this study (ventral part of the pallidum, dorsomedial nucleus of the thalamus and midbrain) and it may be that subsegmentation of these regions would show more specific involvement in these particular subregions.

The habenula is involved in the processing of aversive information. By inhibiting dopamine-releasing neurones, it suppresses motor activity under adverse conditions such as failure to obtain a reward or anticipation of an unpleasant outcome.[8] For example, in a motion-prediction fMRI task the habenula was activated when a subject received feedback indicating that their response was wrong.[9] When the action of the habenula is impaired (such as when it becomes atrophied), it is likely that even though the outcome of an action may be negative, it would be difficult for a subject to avoid the action. This may be expressed as abnormal reward behaviours similar to those seen in bvFTD including increased impulsivity, binge eating and alcohol or recreational drug abuse.

There are some limitations to this study. Owing to the small dimensions of the nucleus and the resolution of the MRI, it was not possible to distinguish between the lateral and medial habenula, and specifically locate the involvement within the nucleus. The small sample size did not allow us to further differentiate among the different genetic mutations in FTD and their potential different impact. Moreover, we did not systematically collect information about behaviours linked to reward processing, preventing us from investigating any possible correlation

with the clinical symptoms. Further studies in larger genetic and pathologically confirmed cohorts are required to confirm the role of the habenula in bvFTD, together with studies aimed at defining the functional and structural connections of the habenula within the reward network.

In summary, we found that in bvFTD the region with the most atrophy in comparison to controls was the habenula and that this region is uniquely affected in this disorder in comparison with an age-matched AD cohort. We suggest that the habenula is an under-recognised area of importance in bvFTD and may be a key region involved in the development of abnormal reward processing.

Martina Bocchetta,[1,2,3] Elizabeth Gordon,[1] Charles R Marshall,[1] Catherine F Slattery,[1] M Jorge Cardoso,[1,4] David M Cash,[1,4] Miklos Espak,[1,4] Marc Modat,[1,4] Sebastien Ourselin,[1,4] Giovanni B Frisoni,[2,5] Jonathan M Schott,[1] Jason D Warren,[1] Jonathan D Rohrer[1]

[1]Department of Neurodegenerative Disease, Dementia Research Centre, UCL Institute of Neurology, London, UK
[2]Laboratory of Alzheimer's Neuroimaging and Epidemiology, IRCCS Istituto Centro San Giovanni di Dio—Fatebenefratelli, Brescia, Italy
[3]Department of Molecular and Translational Medicine, University of Brescia, Brescia, Italy
[4]Translational Imaging Group, Centre for Medical Image Computing (CMIC), University College London, London, UK
[5]Memory Clinic and Laboratory of Neuroimaging of Aging, University Hospitals and University of Geneva, Geneva, Switzerland

Correspondence to Dr Jonathan D Rohrer, Dementia Research Centre, Department of Neurodegenerative Disease, UCL Institute of Neurology, 8–11 Queen Square, London WC1N 3BG, UK; j.rohrer@ucl.ac.uk

PostScript

OPEN ACCESS

CrossMark

REFERENCES

1 Haber SN, Knutson B. The reward circuit: linking primate anatomy and human imaging. *Neuropsychopharmacology* 2010;35:4–26.
2 Perry DC, Sturm VE, Seeley WW, et al. Anatomical correlates of reward-seeking behaviours in behavioural variant frontotemporal dementia. *Brain* 2014;137(Pt 6): 1621–6.
3 Hikosaka O, Sesack SR, Lecourtier L, et al. Habenula: crossroad between the basal ganglia and the limbic system. *J Neurosci* 2008;28:11825–9.
4 Benarroch EE. Habenula: recently recognized functions and potential clinical relevance. *Neurology* 2015;85:992–1000.
5 Savitz JB, Nugent AC, Bogers W, et al. Habenula volume in bipolar disorder and major depressive disorder: a high-resolution magnetic resonance imaging study. *Biol Psychiatry* 2011;69:336–43.
6 Lawson RP, Drevets WC, Roiser JP. Defining the habenula in human neuroimaging studies. *Neuroimage* 2013;64:722–7.
7 Rohrer JD, Nicholas JM, Cash DM, et al. Presymptomatic cognitive and neuroanatomical changes in genetic frontotemporal dementia in the Genetic Frontotemporal dementia Initiative (GENFI) study: a cross-sectional analysis. *Lancet Neurol* 2015;14:253–62.
8 Hikosaka O. The habenula: from stress evasion to value-based decision making. *Nat Rev Neurosci* 2010;11:503–13.
9 Ullsperger M, von Cramon DY. Error monitoring using external feedback: specific roles of the habenular complex, the reward system, and the cingulate motor area revealed by functional magnetic resonance imaging. *J Neurosci* 2003;23:4308–14.

SUPPLEMENTARY DATA

Imaging methods

Volumetric T1-weighted MRI was performed in all 45 subjects on a 3T scanner (Tim Trio, Siemens) with the following parameters: TR=2200ms, TI=900ms, TE=2.9ms, flip angle=10°, acquisition matrix=256x256 and spatial resolution=1.1mm. Raw T1-weighted images were transformed into standard space by a rigid registration to the Montreal Neurological Institute (MNI305) template,[10-12] using NiftyReg, revision #418 (Centre for Medical Image Computing, UCL: http://cmic.cs.ucl.ac.uk/home/software/).

Segmentations of the habenula were then performed manually on coronal slices of a volumetric T1-weighted MRI using NiftyMIDAS (Centre for Medical Image Computing, UCL: http://cmic.cs.ucl.ac.uk/home/software/) using the protocol as described below. The intrarater intraclass correlation coefficient for this segmentation protocol was 0.938 (95% confidence intervals: 0.771-0.984) and 0.909 (0.677-0.977) for left and right habenula respectively, tested in a sample of ten cognitively-normal controls, scanned using the same MRI protocol as the study participants. Dice overlapping and Jaccard similarity coefficient indexes were 0.83 (standard deviation 0.06) and 0.71 (0.08) respectively. Volumes of the habenula were computed from the manual segmentations performed in NiftyMIDAS.

In order to obtain volumes for the rest of the brain we performed a cortical parcellation using a multiatlas segmentation propagation approach following the brainCOLOR protocol combining regions of interest to calculate grey matter volumes of the entire cortex, separated into the frontal, temporal, parietal, occipital, cingulate, and insula cortices.[13] We also performed a subcortical parcellation using the Neuromorphometrics protocol for the hippocampus, amygdala, caudate,

putamen, pallidum, nucleus accumbens, thalamus and brainstem and a parcellation of the cerebellum using the Diedrichsen cerebellar atlas producing a measure for the entire cerebellum by combining regions of interest.[13]

All brain volumes were corrected for total intracranial volume (TIV), which was calculated using the Statistical Parametric Mapping (SPM) 12 software, version 6225 (www.fil.ion.ucl.ac.uk/spm), running under Matlab R2012b (Math Works, Natick, MA, USA). The TIV corrected volume of a specific structure for each subject "i" was computed as follows: Structure $volume_{corrected(i)}$ = Structure $volume_{raw(i)} * TIV_{mean} / TIV_{(i)}$, where "Structure $volume_{raw(i)}$" is the raw value of the structure of the subject "i", "TIV_{mean}" is the average TIV of the study group, and "$TIV_{(i)}$" is the TIV of the subject "i".

Detailed segmentation protocol for the habenula on 3T MRI

1. Introduction

This protocol describes how to manually segment the human habenula on volumetric T1-weighted magnetic resonance images (MRIs), combining the criteria described by Savitz et al., 2011 [5] and by Lawson et al., 2013 [6] (Supplementary Figure). The habenula contains relatively dense white matter plexuses, so it can be distinguished from the adjacent gray matter nuclei by its contrast (i.e. hyper-intensity) on MRI.

2. Segmentation procedures

2.1 Image Orientation/Registration/Standard space

The segmentations are made on MRIs rigidly registered to Montreal Neurological Institute (MNI) standard space.

2.2 Direction of segmentation

Segmentation proceeds on contiguous coronal slices in the caudo-rostral direction. For a slice thickness of 1 mm, approximately 4-5 slices include the habenula (Supplementary Figure).

3. Segmentation landmarks

The segmentation includes the lateral and medial habenular nuclei, which could not be reliably distinguished from each other and thus are combined into a single habenular region.

3.1 Most caudal slice

The habenular segmentation begins on the caudal slice containing the posterior commissure (or the habenular commissure), in which the habenula is present as opposed to cerebrospinal fluid or the most rostral extent of the pineal gland. The habenula is clearly evident as a pyramidal-shaped structure which bulges into the third ventricle along the ventromedial aspect of the thalamus.

3.2 Most rostral slice

The habenular segmentation ends at the most rostral slice where the bright habenular tissue is not visible as protruding into the cerebrospinal fluid of the third ventricle, while it appears the dorsal tip of the stria medullaris (the white matter track which delimits the ventromedial aspect of the medial thalamus). In this slice, the habenula is not visible as delimited ventrally and medially from the thalamus by the stria medullaris of thalamus.

3.3 Ventral boundary

In the most caudal slices, the ventral boundary is defined by the dorsal edge of the white matter of the posterior commissure (or the habenular commissure). In the most rostral slices, the habenula borders with the paraventricular nucleus of the thalamus.

3.4 Dorso-lateral boundary

The dorsal and lateral borders are defined by the mediodorsal thalamic nucleus, limitans nucleus or pretectal area in most caudal slices, and by the white matter of the stria medullaris of the thalamus in the rostral slices.

3.5 Medial boundary

The cerebrospinal fluid of the third ventricle is the prominent landmark to define the medial boundary of the habenula.

Supplementary Figure. Example of habenular segmentation on the ICBM152 2009c Nonlinear Symmetric - 1x1x1mm template (McConnell Brain Imaging Centre, Montreal

Neurological Institute, McGill University). All 1 mm slices are shown, in the caudo-rostral direction.

Caudal ⟶ Rostral
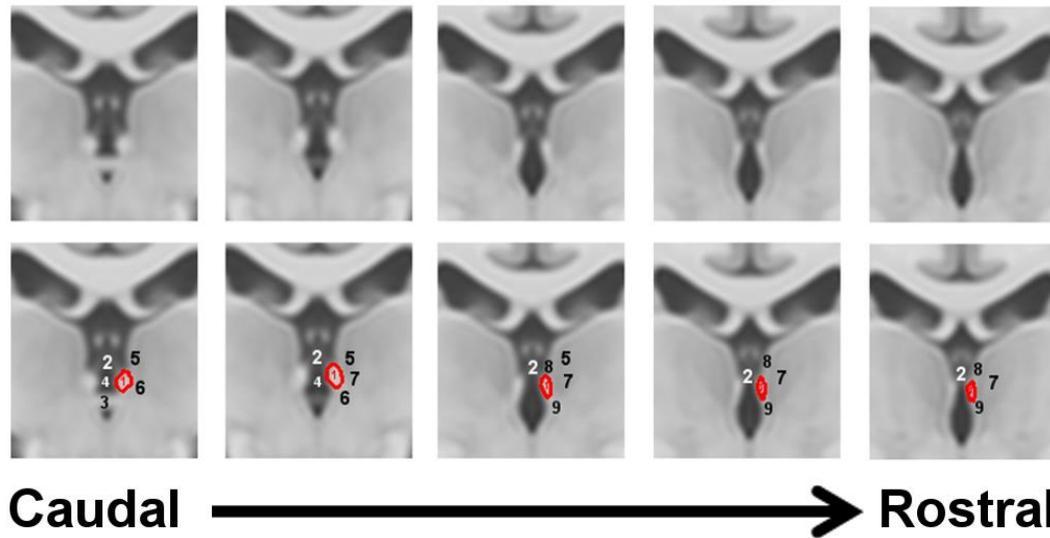
1- Habenula
2- Third ventricle
3- Posterior commissure
4- Habenular commissure
5- Mediodorsal thalamic nucleus
6- Limitans nucleus / Pretectal area
7- Ventromedial thalamic nucleus
8- Stria medullaris
9- Paraventricular thalamic nucleus

Supplementary Table. Volumetry of brain structures in 15 patients with bvFTD and 15 healthy control participants. Volumes are corrected for TIV. Values denote mean (standard deviation) volumes in mm³. p-values denote significance on Mann-Whitney U test. *denotes significance after correction for multiple comparisons.

		bvFTD (n=15)	Control (n=15)	p-value (*bvFTD vs Ctrl*)	% difference (*bvFTD vs Ctrl*)
Habenula	**Right**	16 (3)	23 (2)	**<0.001***	30%
	Left	17 (2)	24 (2)	**<0.001***	28%
Frontal Cortex	**Right**	79850 (4699)	89306 (5454)	**<0.001***	11%
	Left	77130 (3817)	86667 (5570)	**<0.001***	11%
Temporal Cortex	**Right**	49270 (6741)	58717 (2766)	**<0.001***	16%
	Left	48265 (7676)	58919 (3158)	**<0.001***	18%
Insula Cortex	**Right**	5298 (684)	6918 (703)	**<0.001***	23%
	Left	5339 (791)	7263 (623)	**<0.001***	26%
Cingulate Cortex	**Right**	11270 (1138)	12405 (1123)	**0.029**	9%
	Left	12217 (872)	13727 (1273)	**<0.001***	11%
Parietal Cortex	**Right**	43906 (3592)	47309 (3513)	**0.019**	7%
	Left	44204 (2984)	47398 (4572)	**0.037**	7%
Occipital Cortex	**Right**	35453 (2235)	36857 (2988)	0.285	4%
	Left	33984 (1873)	35475 (2640)	0.074	4%
Hippocampus	**Right**	3645 (892)	4636 (486)	**0.001***	21%
	Left	3361(784)	4397 (337)	**<0.001***	24%
Amygdala	**Right**	731 (237)	971 (108)	**0.003***	25%
	Left	708 (206)	1015 (119)	**<0.001***	30%
Caudate	**Right**	3231 (620)	3526 (370)	**0.037**	8%
	Left	2944 (568)	3341(404)	**0.011**	12%
Putamen	**Right**	4290 (620)	4857 (560)	**0.004**	12%
	Left	4268 (579)	4872 (613)	**0.008**	12%
Pallidum	**Right**	803 (119)	850 (72)	0.267	5%
	Left	814 (118)	883 (98)	0.089	8%
Nucleus accumbens	**Right**	517 (103)	693 (65)	**<0.001***	25%
	Left	531 (131)	757 (77)	**<0.001***	30%
Thalamus	**Right**	5457 (675)	6351 (471)	**<0.001***	14%
	Left	5256 (646)	6206 (419)	**<0.001***	15%
Brain Stem		9109 (911)	9942 (647)	**0.009**	8%
Cerebellum		100761 (10296)	107356 (7454)	0.074	6%

Additional references for Supplementary Data

10. Evans AC, Collins DL, Milner B. An MRI-based stereotaxic atlas from 250 young normal subjects. Proc 22nd Annual Symposium, Society for Neuroscience. 1992; 18:408.

11. Evans AC., Marrett S, Neelin P, Collins L, Worsley K, Dai W. et al. Anatomical mapping of functional activation in stereotactic coordinate space. NeuroImage. 1992; 1:43-63.

12. Evans AC, Collins DL, Mills SR, Brown ED, Kelly RL, Peters TM. 3D statistical neuroanatomical models from 305 MRI volumes. Proc IEEE Nuclear Science Symposium and Medical Imaging Conference. 1993;1813-1817.

13. Cardoso MJ, Modat M, Wolz R, Melbourne A, Cash D, Rueckert D, Ourselin S. Geodesic information flows: spatially-variant graphs and their application to segmentation and fusion. IEEE TMI 2015, doi: 10.1109/TMI.2015.2418298.